*Semiconductor Physics, Quantum Electronics & Optoelectronics, 2017. V. 20, N 3. P. 305-313.*
doi: https://doi.org/10.15407/spqeo20.03.305

PACS 78.55.Et, 78.55.-m

# On determination of $Cd_{1-x}Zn_xTe$ composition from an analysis of the 4.2, 77 and 295 K edge photoluminescence spectra

**K.D. Glinchuk, V.P. Maslov, O.M. Strilchuk, A.B. Lyapina**
*V. Lashkaryov Institute of Semiconductor Physics, NAS of Ukraine,*
*41, prospect Nauky, 03680 Kyiv, Ukraine*
*Phone: +38(044) 5255098, fax: +38(044) 5253337,*
*e-mail*: strilchuk@isp.kiev.ua

**Abstract.** The known and obtained in this work dependences of the 4.2, 77 and 295 K peak positions $h\nu_m$ of the $Cd_{1-x}Zn_xTe$ edge emission bands induced by: (a) annihilation of free $X$ and bound on shallow neutral acceptors $A^0$ or shallow neutral donors $D^0$ excitons $A^0X$ and $D^0X$ and (b) recombination of free and shallow donor bound electrons with free holes on $Cd_{1-x}Zn_xTe$ composition $x$ ($x \le 0.28$) are analyzed in detail. It is shown that the 4.2 K peak position of the $A^0X$ induced emission band used for the exact $x$ determination could be related with some problems arising from variety of the 4.2 K $h\nu_m(A^0X)$ vs. $x$ dependences. As a result of the pointed problem, analysis of the 4.2 K $h\nu_m(A^0X)$ vs. $x$ dependences permits to find the $x$ value with some inaccuracy (some unknown factors shift the energy position of the $A^0X$ bound exciton are responsible for this fact). The noticeable (differing from the expected theoretical ones) differences of the peak positions of emission bands $h\nu_m$ induced by radiative annihilation of $D^0X$ bound excitons at 295 K, radiative recombination of donor bound electrons $D^0$ with free holes $h$ at 300 K and radiative annihilation of free electrons $e$ and holes at 300 K, *i.e.* of 295 K $h\nu_m(D^0X)$, 300 K $h\nu_m(D^0h)$ and 300 K $h\nu_m(eh)$ values, accordingly, vs. $x$ dependences are observed and briefly analyzed.

**Keywords:** $Cd_{1-x}Zn_xTe$ composition, photoluminescence, free and bound excitons, accuracy of composition determination.

Manuscript received 06.07.17; revised version received 01.08.17; accepted for publication 06.09.17; published online 09.10.17.

## 1. Introduction

Peak positions $h\nu_m$ of the edge emission bands induced by: (a) radiative annihilation of bound (by shallow neutral acceptors $A^0$ or shallow neutral donors $D^0$) $A^0X$ or $D^0X$ excitons (the dissociation paths are $A^0X \rightarrow A^0 + h\nu$ and $D^0X \rightarrow D^0 + h\nu$), (b) radiative transitions of electrons bound neutral shallow donors $D^0$ with the holes $h$ (the dissociation path is $D^0 + h \rightarrow D^+ + h\nu$), c) radiative annihilation of free exciton $X$, d) radiative recombinations of free electrons $e$ and holes $h$ in mixed $Cd_{1-x}Zn_xTe$ compounds depend strongly on their chemical composition $x$, *i.e.* on the zinc content $x$ (the $h\nu_m$ values shift to higher energies as $x$ is increased) [1-16][1]. So, the luminescent method – measurements of the 1.6 [8], 2 [4], 4.2 [1, 5, 9, 10, 13], 12 [2], 77 [6], 80 K [3] and room temperature $T = 295…300$ K [2, 7, 11] peak positions of the edge emission bands in principle could be used for finding composition of

[1] In many of the cited works the band gap energy $E_g$ vs. $x$ dependences are given. They were found from the obtained in the experiment peak positions of the exciton (carrier) induced emission $h\nu_m$ vs. $x$ dependences by taking into account exciton (carrier) binding energies. So, in the pointed cases the given below $h\nu_m$ vs. $x$ dependences were plotted from the known $E_g$ vs. $x$ dependences by taking into account the corresponding exciton (carrier) binding energies (see below).

$Cd_{1-x}Zn_xTe$ crystals and films. Obviously, the most convenient for this purpose are measurements of the $h\nu_m$ values at temperatures $T$ = 4.2, 77 and 295…300 K. Below we will analyze the known and obtained in this work (found by an analysis of the $A^0X$, $D^0X$, $D^0h$, $X$ and $e$–$h$ induced emission band) the 4.2, 77 and 295…300 K $h\nu_m$ vs. $x$ dependences for $x$ determination in $Cd_{1-x}Zn_xTe$. In particular the strict analysis of the 4.2, 77 and 300 K bound exciton induced emission bands $A^0X$ and $D^0X$ in $Cd_{1-x}Zn_xTe$ crystals with the different Zn content and various temperatures was a basis for obtaining presented by us the 4.2, 77 and 295 K $h\nu_m(A^0X, D^0X)$ vs. $x$ dependences. We will find the accuracy of the $x$ determination by measuring the 4.2 K $A^0X$ induced luminescence bands and show that the same problems arise, when we use the 4.2 K $h\nu_m(A^0X)$ vs. $x$ dependences for $x$ determination. They results from unexpected variety of the observed 4.2 K $h\nu_m(A^0X)$ vs. $x$ dependences for $Cd_{1-x}Zn_xTe$ crystals. The reasons leading to variety of the 4.2 K $h\nu_m(A^0X)$ vs. $x$ dependences are discussed. We also discuss the notable unexpected difference of the 295 K $h\nu_m(D^0X)$, 300 K $h\nu_m(D^0h)$ and 300 K $h\nu_m(eh) = \varphi(x)$ calibration curves. Finally, in the Appendix obtained by us photoluminescence characteristics of $A^0X$ and $D^0X$ induced emission bands in $Cd_{1-x}Zn_xTe$ crystals ($x \le 0.28$ and $T$ = 4.2 – 295 K) will be presented (peak emission intensities, emission peak positions and half-widths of $A^0X$ and $D^0X$ induced emission bands will be given). These data will be helpful for identification of the $A^0X$ and $D^0X$ induced emission bands in the $Cd_{1-x}Zn_xTe$ crystals with moderate $x$ (≤0.28) and $T$ (4.2–295 K) value.

## 2. Experimental

Semi-insulating, *i.e.* the specific resistivity $\rho \ge 10^5$ Ohm·cm at $T \le 295$ K ($\rho \approx 3\cdot10^9$ Ohm·cm) at room temperature and $\rho \to \infty$ at $T \le 77$ K for crystals with $x = 0.1$, $Cd_{1-x}Zn_xTe$ crystals with the known $x$ values 0, 0.04, 0.1, 0.2 and 0.28 ($x$ = 0.04 and 0.1 were found by the X-ray diffraction measurements and $x$ = 0.2 and 0.28 – by the X-ray spectral microanalysis) were used to find the given below 4.2, 77 and 295 K $h\nu_m(A^0X, D^0X)$ vs. $x$, $1/T$ dependences from the analysis of corresponding edge emission spectra. Luminescence was excited using the He-Ne laser (energy $h\nu$ = 1.96 eV, the excitation intensity $L = 10^{18}$ quanta/cm$^2$·s). The MDR-23 spectrometer was used to analyze (with inaccuracy ±0.2 meV at 4.2 K and ±1 meV at 295 K) the photoluminescence spectra (the line-shapes of the $A^0X$ and $D^0X$ emission bands (their peak positions $h\nu_m$ and half-widths $w$) were found). The $h\nu_m$ values for the examined emission bands did not depend on the intensity of photoluminescence excitation. Before photoluminescence measurements, the $Cd_{1-x}Zn_xTe$ crystals were polished in a bromide-methanol etchant.

## 3. Results and discussion

### *3.1. The 4.2 K $h\nu_m$ vs. $x$ dependences*

Fig. 1 illustrates the known (see [1, 5, 9, 10, 13]) and obtained in this work the 4.2 K $h\nu_m(A^0X)$, $h\nu_m(D^0X)$ and $h\nu_m(X)$ vs. $x$ dependences for determination of $Cd_{1-x}Zn_xTe$ composition. Below, we shall discuss in detail the origin (identification) of radiative transitions responsible for above pointed 4.2 K $h\nu_m$ vs. $x$ calibration dependences.

(a) *The 4.2 K peak position of the $A^0X$ induced emission $h\nu_m(A^0X)$ vs. $x$ calibration dependences.* 1) The 4.2 K $E_g$ vs. $x$ dependences ($x \le 0.065$) are given in [5, 10]. They were found by adding the $A^0X$ exciton binding energy $\varepsilon_{bA}$ =16 meV to the measured $h\nu_m(A^0X)$ vs. $x$ dependences (it is assumed that $\varepsilon_{bA} \ne \varphi(x)$). So, the given in [5, 10] band gap $E_g$ vs. $x$ dependences were replotted by us into primary dependences $h\nu_m(A^0X) = E_g - \varepsilon_{bA}$ vs. $x$ ($x \le 0.065 - 0.07$) by taking into account the $\varepsilon_{bA}$ value. They are shown in Fig. 1, curves *1*, *2* and *2′*. 2) The 4.2 K $h\nu_m(A^0X)$ vs. $x$ calibration dependences are also given in [1,9] and presented in Fig. 1 (curves *3* and *4*). Obtained by us 4.2 K $h\nu_m(A^0X)$ vs. $x$ dependence is given in Fig. 1 (see the curves *5*), too. This dependence is really the 4.2 K $h\nu_m(A^0X)$ vs. $x$ dependence as follows, on the one hand, from the coincidence for crystal with $x$ = 0 of the observed 4.2 K $h\nu_m$ value 1.590 eV with the 4.2 K $h\nu_m(A^0X)$ value, and, on the other hand, with the observed rather high half-width of emission band analyzed[2]. In the inset of Fig. 1, the 4.2 K line shapes of the $A^0X$ induced emission bands in $Cd_{1-x}Zn_xTe$ crystals are shown ($h\nu_m$ = 1.613 eV and $w$ =3.6 meV for a crystal with $x$ = 0.04 and $h\nu_m$ = 1.654 eV and $w$ = 11.6 meV for a crystal with $x$ = 0.2). Note that given here and in the Appendix 4.2 K $h\nu_m(A^0X)$ vs. $x$ dependences could be used to identify the 4.2 $A^0X$ induced emission band in $Cd_{1-x}Zn_xTe$ crystals with moderate $x$ values. The 4.2 K line shapes of the $A^0X$ induced emission band in $Cd_{1-x}Zn_xTe$ crystals with different $x$ values are also given in the Appendix.

(b) *The 4.2 K peak position of the $D^0X$ induced emission band $h\nu_m$ ($D^0X$) vs. $x$ calibration curve.* The obtained by us 4.2 K $h\nu_m(D^0X)$ vs. $x$ calibration curve is given in Fig. 1 (curve *6*). The $D^0X$ identification of the pointed emission was made on the basis of its 4.2 K peak position for this band at $x$ = 0 (1.594 eV, it coincides with the known 4.2 K $h\nu_m(D^0X)$ value at $x$ = 0) and its

[2] The $A^0X$ induced emission band in 4.2 K $Cd_{1-x}Zn_xTe$ edge luminescence spectrum could be identified due to its comparatively high half-width as compared with the corresponding for the $D^0X$ induced emission band (see, for example, [1, 11, 14, 17] and below). In addition to the stated, some other arguments how to identify the $A^0X$ induced emission band in the 4.2 K $Cd_{1-x}Zn_xTe$ edge luminescence spectrum, when in it only one of two excitonic emission bands are observed are given in [15, 16].

rather small at low $x$ 4.2 K half-width $w$ = 0.3 meV [15, 16]. The 4.2 K line shapes of the $D^0X$ induced emission bands in $Cd_{1-x}Zn_xTe$ crystals are given in the inset of Fig. 1: $h\nu_m$ = 1.617 eV and $w$ =1.5 meV for a crystal with $x$ = 0.04 and $h\nu_m$ = 1.667 eV and $w$ = 4.7 meV for a crystal with $x$ = 0.2. The 4.2 K line shapes of the $D^0X$ induced emission bands for crystals with different $x$ values are also given in Appendix. Given here and in the Appendix 4.2 K $h\nu_m(D^0X)$ vs. $x$ dependences could be used to identify the 4.2 K induced emission band in $Cd_{1-x}Zn_xTe$ crystals with moderate $x$ values.

(c) *The 4.2 K peak position of the free exciton induced emission $h\nu_m(X)$ vs. $x$ calibration dependence.* In [13] $E_g$ vs. $x$ calibration dependence ($x \le 0.055$) is given. It was obtained by adding to the found 4.2 K $h\nu_m(X)$ vs. $x$ dependence the free exciton binding energy $\varepsilon_X$ = 10 meV. So, the given in [13] $E_g$ vs. $x$ dependence was replotted by us into $h\nu_m(X) = \varphi(x)$ primary dependence $h\nu_m(X) = E_g(x) - \varepsilon_X$ vs. $x$ ($x \le 0.05$) by taking into account the $\varepsilon_X$ value. Then, thus obtained the 4.2 K peak position of the free exciton induced emission band $h\nu_m(X)$ vs. $x$ calibration dependence is given in Fig. 1, curve 4 (no convenient form of the 4.2 K free exciton induced emission band is given it [13]).

Naturally, in principal all the shown in Fig. 1 4.2 K dependences $h\nu_m(X)$, $h\nu_m(A^0X)$ and $h\nu_m(D^0X)$ on $x$ could be used to find the $x$ value, if the $A^0X$, $D^0X$ and $X$ induced emission bands are reliably identified in the excitonic luminescence spectra. But some difficulties arise, when one tries to use for $x$ determination the 4.2 K peak position of the $A^0X$ induced emission band vs. $x$ dependences. Really, the shown in Fig. 1 4.2 K $h\nu_m(A^0X)$ vs. $x$ dependences obtained by different authors somewhat strongly differ, *i.e.* a number of 4.2 K $h\nu_m(A^0X)$ vs. $x$ dependences are observed. Naturally, the stated above will result in variety of $x$ values for the fixed 4.2 K $h\nu_m(A^0X)$ value. It mainly refers to the $Cd_{1-x}Zn_xTe$ crystals with the low Zn content ($x \le 0.065$). Really, for example, if the measured 4.2 K $h\nu_m$ value is 1.62 eV, then $x$ = 0.056 as it follows from the 4.2 K $h\nu_m(A^0X)$ vs. $x$ dependences given by the curves *1*, *2*, *2′* of Fig. 1, and $x = 0.09 \pm 0.01$, if the 4.2 K $h\nu_m(A^0X)$ vs. $x$ dependences given by the curves *3* to *5* in Fig. 1 are used for $x$ determination. So, if one uses for $x$ determination the 4.2 K $h\nu_m(A^0X)$ vs. $x$ dependences given in [1, 5, 9, 10], the obtained $x$ value is $x = x_0 + \Delta x = 0.073 \pm 0.012$ ($x_0$ is the average $x$ value and $\Delta x$ is deviation of the $x$ value from the average one), *i.e.* is found with a rather low accuracy (the relative inaccuracy of $x$ determination $\Delta x/x_0 \approx \pm 23\%$ is rather large). So, only rough estimates of the low (≤0.06) $x$ values could be made by using the given in [1, 5, 9, 10] (see the curves *1* to *4*) 4.2 K $h\nu_m(A^0X)$ vs. $x$ dependences. On the contrary, for crystals with a moderate Zn content ($x$ = 0.065…0.28) the relative inaccuracy of $x$ determination is rather small (±5%) due to a small difference at the pointed $x$ values of the 4.2 K $h\nu_m(A^0X)$ vs. $x$ dependences found in [1, 9] (see curves *3* and *4*) and in this work (see curve *5*). For example, if the measured 4.2 K $h\nu_m$ vs. $x$ value is 1.65 eV, then the obtained $x$ values are 0.18 and 0.20, *i.e.* $x = 0.19 \pm 0.01$, and a relative inaccuracy $\Delta x/x_0$ is ±5%, as it follows from the 4.2 K $h\nu_m$ vs. $x$ dependences given by the curves *3* to *5* in Fig. 1.

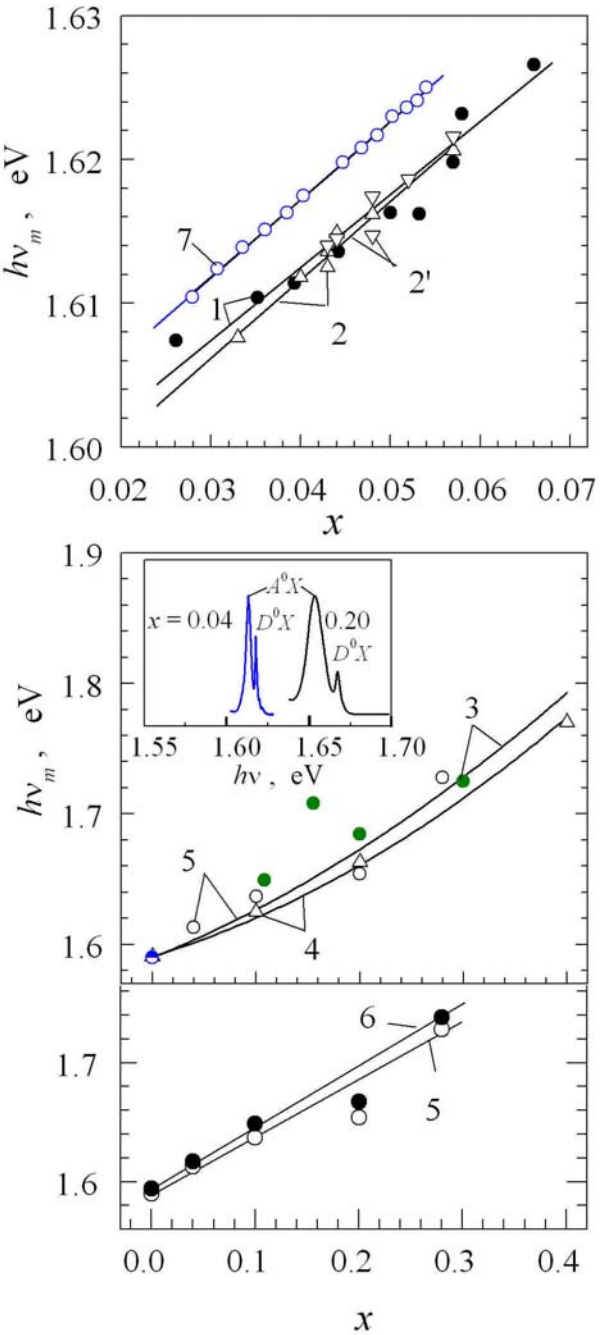


**Fig. 1.** The 4.2 K peak positions of emission bands $h\nu_m$ in $Cd_{1-x}Zn_xTe$ induced by annihilation of: (a) bound excitons $A^0X$ (*1* to *5*), where *1* – data of [5]; *2*, *2′* – data of [10]; *3* – data of [9]; *4* – data of [1]; *5* – data obtained in the present work; (b) $D^0X$ bound excitons (*6* – data obtained in the present work); (c) free excitons $X$ (*7* – data of [13]) vs. $Cd_{1-x}Zn_xTe$ composition $x$ are given. In the inset, the 4.2 K line shapes of emission bands induced in the studied $Cd_{1-x}Zn_xTe$ crystals by annihilation of $A^0X$ and $D^0X$ bound excitons are given (the corresponding $h\nu_m$ and $w$ values are given in the text).

Now, we will discuss the possible reasons leading to a difference in the observed 4.2 K $h\nu_m(A^0X)$ vs. $x$ dependences, *i.e.* to different energy positions of the $A^0X$ bound exciton at a given $x$. We do not think the main reason leading to a discussed differences of the 4.2 K $h\nu_m(A^0X)$ vs. $x$ dependences is a different origin of the $A^0$ constituents in the $A^0X$ bound exciton, *i.e.* the stated above could be hardly related with the different origin of shallow acceptors $A^0$ that are constituents of the $A^0X$ complexes. Really, the observed difference in the discussed 4.2 K $h\nu_m(A^0X)$ vs. $x$ dependences is usually greater than the expected one, if one analyze the possible shift of the $A^0X$ bound exciton energy position due to different $A^0$ constituents [15, 18-20]. The effect of different $A^0$ constituents of the $A^0X$ complexes on the 4.2 K $h\nu_m(A^0X)$ value in CdTe and ZnTe compounds are given in [15, 18-20]; as one can see, usually the different $A^0$ constituents of $A^0X$ complexes could only relatively weakly influence the 4.2 K peak position of the $A^0X$ induced emission band in CdTe and ZnTe and most probably in $Cd_{1-x}Zn_xTe$, too.

We think that a row of not exactly known factors mainly influence the 4.2 K peak position of the $A^0X$ induced emission band in $Cd_{1-x}Zn_xTe$. Apparently, these factors are related with the crystal perfection and structural defects [14, 21], compositional disorder [22], crystalline quality [23] and other [12][3]. These factors could differ in various crystals. As a result, a number of 4.2 K $h\nu_m$ values at fixed $x$ values for the emission band induced by annihilation of $A^0X$ complexes appear. So, variety of the 4.2 K $h\nu_m$ vs. $x$ dependences are observed as a result of some feebly controlled factors influencing the peak position of the $A^0X$ induced emission band. A further work is needed to elucidate reasons leading to different $A^0X$ induced 4.2 K $h\nu_m$ values at a given $x$.

### *3.2. The 77 K $h\nu_m(D^0X)$ vs. x calibration curve*

Fig. 2 shows the found in this work dependence of the 77 K peak position of emission induced by annihilation of $D^0X$ bound exciton vs. the zinc content $x$ in $Cd_{1-x}Zn_xTe$ crystals. The $D^0X$ emission band dominates in the 77 K $Cd_{1-x}Zn_xTe$ emission spectra (see also the Appendix). In the experiment, 77 K $h\nu_m(D^0X) =$ 1.5839 eV at $x = 0$. The 77 K line shapes of the $D^0X$ induced emission bands are shown in the inset of Fig. 2: $h\nu_m(D^0X) =$ 1.6372 eV and $w(D^0X) =$ 13.8 meV for a crystal with $x = 0.1$ and $h\nu_m(D^0X) =$ 1.6543 eV and $w(D^0X) =$ 15.8 meV for a crystal with $x = 0.2$. Thereof, the pointed 77 K line-shapes could be used to identify

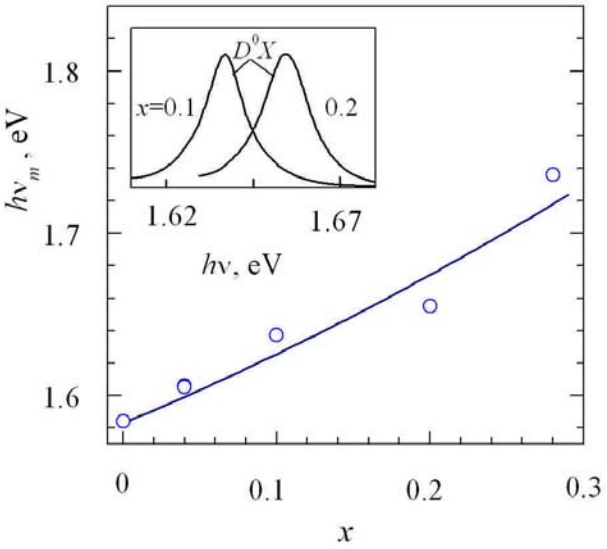


**Fig. 2.** The 77 K peak positions of the $D^0X$ induced emission bands vs. $x$ dependence in $Cd_{1-x}Zn_xTe$ crystals. In the inset, the 77 K line shapes of the $D^0X$ induced emission band in $Cd_{1-x}Zn_xTe$ crystals is shown (the corresponding $h\nu_m$ and $w$ values are given in the text).

the 77 K $D^0X$ induced emission band in $Cd_{1-x}Zn_xTe$ crystals with moderate $x$ values[4].

### *3.3. 295–300 K $h\nu_m$ vs. x calibration curves*

The known and found by us the 293…300 K $h\nu_m$ vs. $x$ calibration curves are as follows in their origin (see Fig. 3) [2, 7, 11].

(a) *The 295 K $h\nu_m(D^0X)$ vs x calibration dependence.* The 295 K peak positions of the $D^0X$ induced emission band $h\nu_m(D^0X)$ vs $x$ calibration curve found in this work is given in Fig. 3 (curve *1*). In the experiment, 295 K $h\nu_m(D^0X) =$ 1.5025 eV at $x = 0$. The 295 K line-shape of the $D^0X$ induced emission band at different $x$ are given in Fig. 3, inset and in the Appendix: $h\nu_m =$ 1.537 eV and $w =$ 41.3 meV for $x = 0.1$, and $h\nu_m =$ 1.567 eV and $w =$ 41 meV for $x = 0.2$. The given line shapes at 295 K for the induced emission band in $Cd_{1-x}Zn_xTe$ crystals with moderate $x$ value could be used to identify the pointed edge emission band in $Cd_{1-x}Zn_xTe$ crystals widely used for detector fabrication [12][5].

[3] Naturally, the pointed factors depend substantially on the $Cd_{1-x}Zn_xTe$ growth technology (or its details, if growth technology is near by the same) that could differ significantly in various laboratories, *i.e.* they are technology dependent.

[4] In [6], the data about 77 K PBE (principal bound exciton) induced emission in $Cd_{1-x}Zn_xTe$ crystals with different zinc content were given. In principle the 77 K $h\nu_m$(PBE) vs. $x$ dependence could be found from the pointed data. But the use of the given in [6] data about PBE induced exciton bands in crystals with different $x$ could be hardly used for $x$ determination as no exact identification of the origin of the PBE induced emission was given in [6]. So, no 77 K $h\nu_m$(PBE) vs. $x$ dependence is given by us.

[5] Note that the 300 K line-shapes of the edge emission induced by radiative transitions are given in [24].

*Semiconductor Physics, Quantum Electronics & Optoelectronics, 2017. V. 20, N 3. P. 305-313.*
doi: https://doi.org/10.15407/spqeo20.03.305

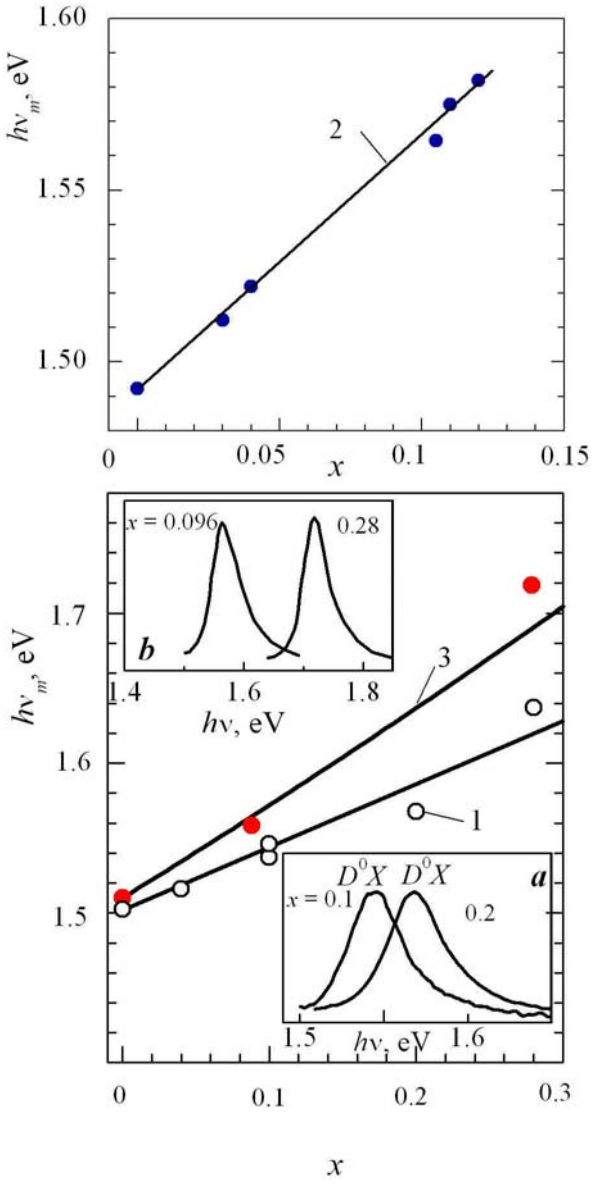


**Fig. 3.** The peak positions of the emission bands $h\nu_m$ induced by: (a) annihilation of bound exciton $D^0X$ at 295 K (1) (the data obtained in these work); (b) $D^0 \to h$ transitions at $T$ = 300 K (2); (c) $e \to h$ recombination at 300 K (*3*) vs. $x$ dependences in $Cd_{1-x}Zn_xTe$ crystals. In the inset: (a) the 295 K line shapes of the $D^0X$ emission band; (b) the 300 K line shapes of the $e \to h$ induced emission band in $Cd_{1-x}Zn_xTe$ crystals with different $x$ are given ( the corresponding $h\nu_m$ and $w$ values are shown in the text).

(b) *The 293–300 K $h\nu_m(D^0 \to h)$ vs x calibration dependence.* The 300 K band gap $E_g$ vs $x$ dependence is really given in [7]. It was obtained the $\varepsilon_d$ value by adding to the really measured 300 K peak positions of emission induced by radiative annihilation of shallow donor bound electrons (the donor ionization energy $\varepsilon_d$ = 0.013 eV) with free holes $h$ (by $D^0 \to h$ radiative transitions). So, the given in Fig. 3 (curve *2*) 300 K peak position of emission induced by $D^0 \to h$ transitions $h\nu_m(D^0 \to h)$ was obtained by subtracting the $\varepsilon_d$ value from the given in [7] $E_g$ vs $x$ dependence. No convenient 300 K line shapes of $D^0h$ induced emission band was given in [7].

(c) *The 300 K $h\nu_m(e \to h)$ vs x calibration dependence.* The 300 K peak positions of the emission induced by recombination of free electrons and holes ($e \to h$ transitions) $h\nu_m(e \to h)$ vs. $x$ calibration dependence is really given in [2] and is replotted in Fig. 3. The 300 K line shape of the *eh* induced emission band shown in the inset *b* of Fig. 3. As can be shown, the main contribution to the 300 K peak intensity of the *e–h* induced emission band is given by the free charge carriers located inside the conduction and valence bands (at the energy $\varepsilon^* = kT/2$ from the edges of conduction (valence) bands). The free charge carriers concentrations are at maximum inside (the pointed bands).

As a result, the relation 300 K $h\nu_m(eh)$ > 300 K $E_g$ holds, theoretically 300 K $h\nu_m(eh)$ = 300 K $E_g + kT/2$) [15].

Naturally, the pointed in (a), (b) and (c) 293–300 K $h\nu_m$ vs. $x$ calibration curves could be used to find the $x$ value, if the emission bands are reliably identified[6].

(d) *Comparison of the 295 K $h\nu_m(D^0X) = \varphi(x)$, 300 K $h\nu_m(D^0h) = \varphi(x)$ and 300 K $h\nu_m(eh) = \varphi(x)$ calibration dependences in $Cd_{1-x}Zn_xTe$ crystals.* The shapes of the 295 K $h\nu_m(D^0X)$, 300 K $h\nu_m(D^0h)$ and 300 K $h\nu_m(eh)$ vs. $x$ calibration dependences in $Cd_{1-x}Zn_xTe$ crystals notably differ, *i.e.* the 295 K $h\nu_m(D^0X)$, 300 K $h\nu_m(D^0h)$ and 300 K $h\nu_m(eh)$ values depend differently on $x$ (see Fig. 3, curves *1* to *3*). This fact is unexpected. Really, the mentioned 295 K $h\nu_m(D^0X)$, 300 K $h\nu_m(D^0h)$ and 300 K $h\nu_m(eh)$ vs. $x$ variations are mainly determined by the corresponding bandgap $E_g$ vs. $x$ variations. Evidently, at any $x$ and $T$ values $h\nu_m(D^0X) = \varphi(E_g, T, \varepsilon_{bD})$, $h\nu_m(D^0h) = \varphi(E_g, T, \varepsilon_d)$ and $h\nu_m(eh) = \varphi(E_g, T)$, where the donor ionization energy $\varepsilon_d$ and the binding energy of the $D^0X$ exciton $\varepsilon_{bD}$ most probably depend weakly on $x$ ($\varepsilon_{bD} \approx$ 14 meV [14]; undoubtedly, $E_g$ vs. $x$ variations are close to each other at $T$ = 295 and 300 K).

One expects to observe similar (identically dependent on $x$) the 295 K $h\nu_m(D^0X)$, 300 K $h\nu_m(D^0h)$ and 300 K $h\nu_m(eh)$ vs. $x$ calibration dependences. Therefore, a new more precise strict analysis of reason leading to the discussed difference of experimental and theoretical shapes of 295 K $h\nu_m(D^0X)$, 300 K $h\nu_m(D^0h)$ and 300 K $h\nu_m(eh)$ vs. $x$ calibration dependences in needed. May be, this new analysis will explain the observed difference of shapes of 295 K $h\nu_m(D^0X)$, 300 K $h\nu_m(D^0h)$ and 300 K $h\nu_m(eh)$ vs. $x$ calibration dependences[7].

[6] The 300 K $h\nu_m$ vs. $x$ dependence ($h\nu_m$ values characterize the edge emission) is given in [11]. But exact identification of the pointed emission (*i.e.* transitions leading to its appearance) was not made. So, this dependence is not given here.

[7] It is not excluded that some weakly controlled factors influence the 295 K $h\nu_m(D^0X)$, 300 K $h\nu_m(D^0h)$ and 300 K $h\nu_m(eh)$ values, thus leading to some deflection between experimental and theoretical $h\nu_m$ values (see above).

(e) *Comparison of the $h\nu_m(D^0X, A^0X)$ vs. $x$ calibration dependences at $T = 4.2$, 77 and 295 K in $Cd_{1-x}Zn_xTe$ crystals.* Fig. 4 shows the obtained by us (see above) $h\nu_m(D^0X)$ and $h\nu_m(A^0X)$ vs. $x$ calibration dependences in $Cd_{1-x}Zn_xTe$ crystals at $T = 4.2$, 77 and 295 K. As one can see, the shapes of the mentioned $h\nu_m(D^0X, A^0X)$ calibration dependences at $T = 4.2$, 77 and 300 K are close to each other, *i.e*. depend weakly on temperature. As it was shown, the shapes of the discussed $h\nu_m(D^0X, A^0X)$ vs. $x$ calibration dependences are mainly determined by the corresponding $E_g$ vs. $x$ variations. It follows from this that the shapes of the bandgap $E_g$ vs. $x$ variations depend weakly on temperature. Obviously, the difference between $h\nu_m(D^0X)$ vs. $x$ dependences at different temperatures is mainly determined by the corresponding differences in the $E_g$ vs. $x$ calibration dependences, *i.e*. at any $x$ 4.2 K $h\nu_m(D^0X)$ – 77 K $h\nu_m(D^0X)$ = 4.2 K $E_g$ – 77 K $E_g$, 4.2 K $h\nu_m(D^0X)$ – 300 K $h\nu_m(D^0X)$ = 4.2 K $E_g$ – 300 K $E_g$ and 77 K $h\nu_m(D^0X)$ – 300 K $h\nu_m(D^0X)$ = 77 K $E_g$ – 300 K $E_g$. Evidently, the difference between the 4.2 K $h\nu_m(D^0X)$ and 4.2 K $h\nu_m(A^0X)$ calibration dependence is close to $\varepsilon_{bA} - \varepsilon_{bD}$ (obviously, $h\nu_m(A^0X) = E_g - \varepsilon_{bA}$ and $h\nu_m(D^0X) = E_g - \varepsilon_{bD}$ at $T = 4.2$ K).

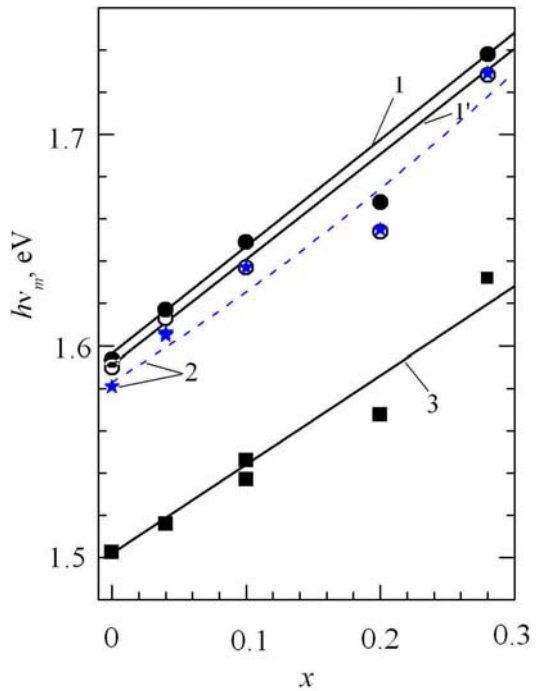


**Fig. 4.** The $h\nu_m(D^0X)$ (*1*–*3*) and $h\nu_m(A^0X)$ (*1′*) vs. $x$ calibration dependences in $Cd_{1-x}Zn_xTe$ crystals at $T = 4.2$ (*1*, *1′*), 77 (*2*) and 295 K (*3*).

## 4. Conclusion

Measurements of the 4.2, 77 and 295–300 K peak position of the edge emission band ($A^0X$, $D^0X$, $D^0h$, $X$ and $e$–$h$ induced) are convenient to find the $Cd_{1-x}Zn_xTe$ composition $x$. But found from the analysis of the 4.2 K $h\nu_m(A^0X)$ vs. $x$ dependences $x$ values are characterized by definite inaccuracies. It is related with some unknown factors influencing the 4.2 K peak position of the $A^0X$ induced emission band (the 4.2 K energy position of $A^0X$ complex). Naturally, pointed results in appearance of a number of 4.2 K $h\nu_m(A^0X)$ vs. $x$ calibration curves for a given set of $x$ values. So, to increase the accuracy of $x$ determination via the analysis of 4.2 K $h\nu_m(A^0X)$ vs. $x$ dependences one needs to find the factors influencing the 4.2 K $h\nu_m(A^0X)$ values, *i.e*., the energy of the 4.2 K $A^0X$ bound exciton. A notable unexpected difference of the 295 K $h\nu_m(D^0X) = \varphi(x)$, 300 K $h\nu_m(D^0h) = \varphi(x)$ and 300 K $h\nu_m(eh) = \varphi(x)$ calibration curves is observed. Maybe, some weakly controlled unknown factors influence the 300 K $h\nu_m(D^0h)$ and 300 K $h\nu_m(eh)$ calibration dependences. Nevertheless, to explain correctly the discussed difference of $h\nu_m(X)$ calibration curves, one need to know the theoretically calculated in a general case the 295 K $h\nu_m(D^0X)$, 300 K $h\nu_m(D^0h)$ and 300 K $h\nu_m(eh)$ values at different $x$ in $Cd_{1-x}Zn_xTe$ crystals.

## Appendix

### Temperature variations of peak emission intensities, emission peak positions and half-widths of the $A^0X$ and $D^0X$ induced luminescence bands in $Cd_{1-x}Zn_xTe$ crystals of difference composition

Here, we pay attention to temperature variations of peak intensities $I$, emission peak positions $h\nu_m$ and half-widths $w$ of the luminescence bands induced by annihilation of $A^0X$ and $D^0X$ bound excitons. The data obtained will permit us to find in $Cd_{1-x}Zn_xTe$ crystals with $x = 0$, 0.04, 0.01, 0.2 and 0.28 the origin of bound excitons that dominate in formation of the 4.2, 77 and 295 K edge emission spectra.

Fig. 5 and 6 show temperature variations of the excitonic part of $Cd_{1-x}Zn_xTe$ edge emission ($x = 0.1$ and 0.2). For the mentioned crystals with $x = 0$, 0.04, 0.01, 0.2 and 0.28, as one can see, both $A^0X$ and $D^0X$ induced emission bands are clearly seen at $T = 4.2$ K (the broad 4.2 K $A^0X$ induced emission band dominates over the rather narrow 4.2 K $D^0X$ induced emission [15-17]). The $D^0X$ induced emission band dominates in the excitonic spectra at $T \geq 30$ K.

Fig. 7 shows temperature variation of peak intensities in the $A^0X$ and $D^0X$ induced emission bands. These emission intensities are nearly constant at low temperatures and are thermally quenched at high temperatures. The thermally induced decrease in the concentrations of neutral shallow acceptors $A^0$ and donors $D^0$ and free excitons $X$, the thermal dissociation of $A^0X$ and $D^0X$ bound excitons are responsible for the above factors. A definite contribution to the discussed emission quenching of $A^0X$ and $D^0X$ emission bands could be given by the non-radiative recombination process of free charge carriers. The discussed quenching is much stronger for the induced emission band, so at

*Semiconductor Physics, Quantum Electronics & Optoelectronics, 2017. V. 20, N 3. P. 305-313.*
doi: https://doi.org/10.15407/spqeo20.03.305

moderate and high temperatures the $D^0X$ induced emission band dominates in the $Cd_{1-x}Zn_xTe$ edge spectrum (the $A^0X$ induced emission band is not observed at high temperatures), see Figs 5 and 6.

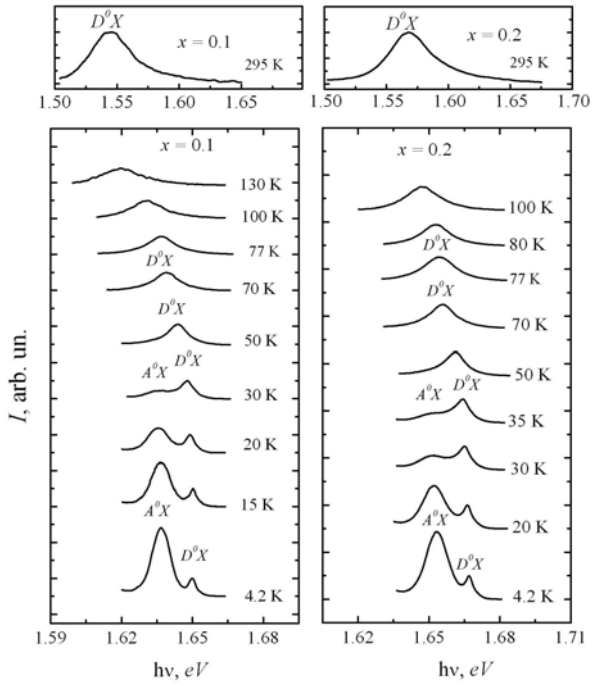


**Fig. 5.** Temperature variations of the excitonic emission spectra in $Cd_{1-x}Zn_xTe$ crystals with $x = 0.1$ and 0.2. Correlation between the emission intensities at different temperatures is arbitrary.

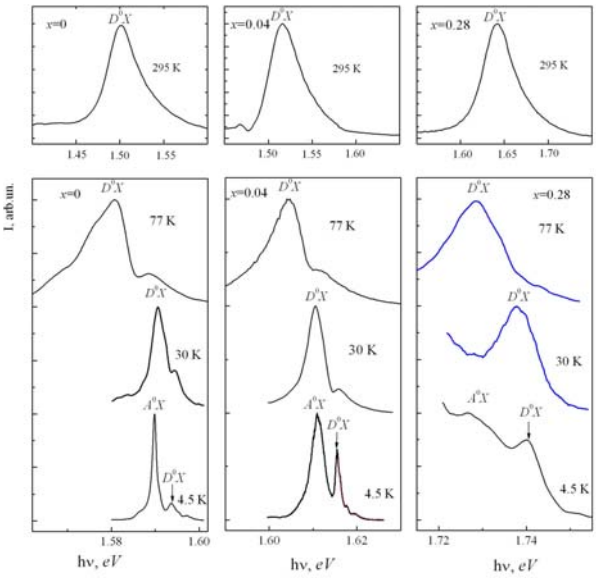


**Fig. 6.** Temperature dependence of the excitonic emission spectra in $Cd_{1-x}Zn_xTe$ crystals with $x = 0$, 0.04 and 0.28. The correlation between the emission intensities for various temperatures is arbitrary.

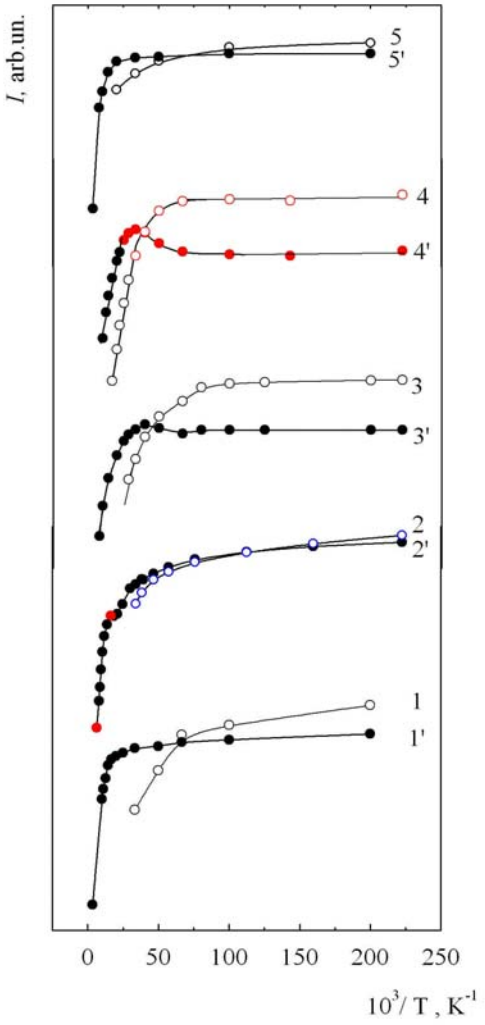


**Fig. 7.** Temperature variations of the peak emission intensities of the $A^0X$ (*1–5*) and $D^0X$ (*1′–5′*) luminescence bands in $Cd_{1-x}Zn_xTe$ crystals with $x = 0$ (*1*, *1′*), 0.04 (*2*, *2′*), 0.1 (*3*, *3′*), 0.2 (*4*, *4′*) and 0.28 (*5*, *5′*). Correlation between $I(A^0X)$ and $I(D^0X)$ values for the same crystals is the real one. Correlation between $I(A^0X)$ and $I(D^0X)$ values in different crystals is arbitrary.

Fig. 8 shows the temperature variation of the peak position of the $A^0X$ and $D^0X$ emission bands $h\nu_m$ in $Cd_{1-x}Zn_xTe$ crystals with $x = 0$, 0.04, 0.01, 0.2 and 0.28. As one can see, the peak positions of the $D^0X$ induced emission bands shift to lower $h\nu_m$ values as the temperature is raised. This temperature shift could be satisfactory described by the following empirical relation (see [17]):

$$h\nu_m(T) = h\nu_m(0) - \frac{AT^2}{T+B}, \qquad \text{(A1)}$$

where $h\nu_m(0)$ is the $h\nu_m$ value at $T = 0$ K ($h\nu_m(0) =$ 1.5937, 1.6141, 1.65, 1.667 and 1.741 eV at $x = 0$, 0.04, 0.01, 0.2 and 0.28, accordingly), $A = 6.48 \cdot 10^{-4}$ eV/K and $B = 264$ K.

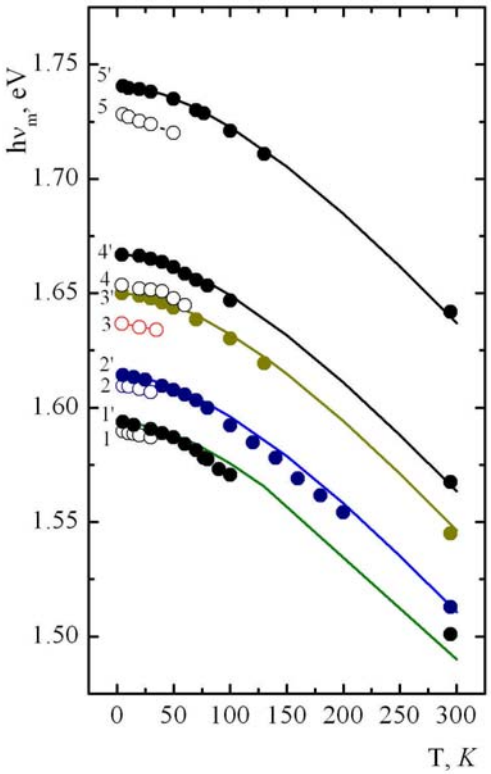


**Fig. 8.** Temperature variations of the peak position $h\nu_m$ of the $A^0X$ (*1*–*5*) and $D^0X$ (*1′*–*5′*) induced emission bands in $Cd_{1-x}Zn_xTe$ crystals of different Zn composition: $x = 0$ (*1*, *1′*), 0.04 (*2*, *2′*), 0.1 (*3*, *3′*), 0.2 (*4*, *4′*) and 0.28 (*5*, *5′*).

As known [17], the mentioned Eq. (A1) describes (is characteristic for) the emission induced by radiative annihilation of $D^0X$ bound excitons, *i.e.*, it describes $h\nu_m$ vs. $T$ variation of the $D^0X$ induced emission band. So, the observed by the coincident of experimental and theoretical 4.2 to 295 K $h\nu_m$ vs. $T$ dependences confirm that the edge (exciton induced) emission band in $Cd_{1-x}Zn_xTe$ crystals with $x = 0$, 0.04, 0.01 and 0.2 is really induced by radiative annihilation of $D^0X$ excitons, *i.e.*, the $D^0X$ induced emission band dominates in the 77 to 295 K edge emission spectra of crystals with $x = 0$, 0.04, 0.01 and 0.2. The dominance of the $D^0X$ induced emission band in the 4.2 to 300 K in $Cd_{1-x}Zn_xTe$ crystals with $x$ lying between 0.07 and 0.14 was noted in [17].

In Fig. 9, the dependences of the half-width $w$ of the $A^0X$ and $D^0X$ induced emission on temperature ($T$ = 4.2…295 K) in $Cd_{1-x}Zn_xTe$ crystals with different Zn content $x$ are given. In Fig. 10, the dependences of the half-width of the $A^0X$ and $D^0X$ induced emission bands $w$ for various temperatures (4.2…295 K) are also given. The shown $w(A^0X, D^0X)$ vs. $x$ and $T$ dependences were obtained from given in Figs 5 and 6 line shapes of the discussed emission bands. As one can see, the $w(A^0X, D^0X)$ values increase, as the temperature and Zn content are raised. It is related with the thermal and alloyed broadening $A^0X$ and $D^0X$ induced emission bands (see, for example, [1, 8]). Thus, the presented $w(x, T)$ curves can be helpful in identification of the $A^0X$ and $D^0X$ induced emission bands in $Cd_{1-x}Zn_xTe$ crystals.

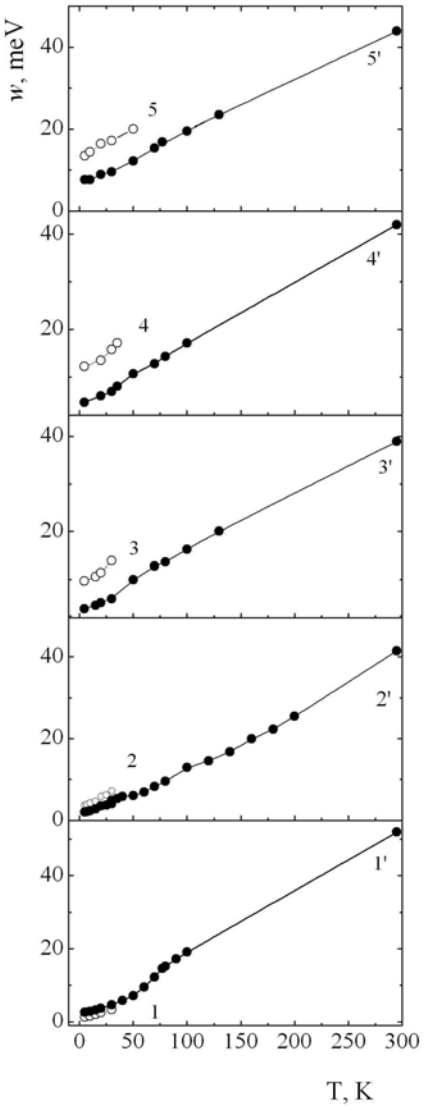


**Fig. 9.** Dependence of the half-width $w$ of the $A^0X$ (*1*–*5*) and $D^0X$ (*1′*–*5′*) induced emission bands on temperature in $Cd_{1-x}Zn_xTe$ crystals with different Zn: $x = 0$ (*1*, *1′*), 0.04 (*2*, *2′*), 0.1 (*3*, *3′*), 0.2 (*4*, *4′*) and 0.28 (*5*, *5′*).

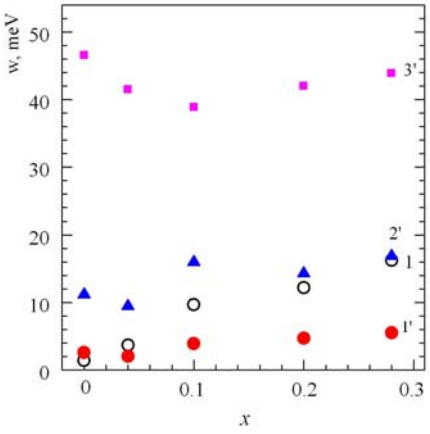


**Fig. 10.** Dependence of the half-width $w$ of the $A^0X$ (*1*) and $D^0X$ (*1′*–*3′*) induced emission bands in $Cd_{1-x}Zn_xTe$ crystals on their Zn composition $x$ at different temperatures $T$: 4.7 (*1*, *1′*), 77 (*2′*) and 295 K (*3′*).

*References*

1. Taguchi T. Crystal growth and neutral acceptor - bound exciton emission of ZnCdTe by THM with Te solvent. *phys. status solidi* (*a*). 1983. **77**, No. 2. P. K115–K119.
2. Olego D.J., Faurie J.P., Sivananthan S., Raccah P.M. Optoelectronic properties of $Cd_{1-x}Zn_xTe$ films grown by molecular-beam epitaxy on GaAs substrates. *Appl. Phys. Lett*. 1985. **47**, No. 11. P. 1172–1174.
3. Lay K.Y., Giles-Taylor N.C., Schetzina J.F., Bochmann K.Y. Growth and characteriozation of CdTe, $Mn_xCd_{1-x}Te$, $Zn_xCd_{1-x}Te$ and $CdSe_yTe_{1-x}$ crystals. *J. Electrochem. Soc*. 1986. **133**, No. 5. P. 1049–1051.
4. Magnea N., Dal'bo F., Poutrat J.L. et al. Molecular beam epitaxial growth of $Cd_{1-x}Zn_xTe$ matched to HgCdTe alloys. *Mater. Res. Soc. Symp. Proc.* 1987. **90**. P. 455–462.
5. Duncan W.M., Koestner R.J., Tregilgas J.H. et al. Non-destructive compositional and defect characterization of CdZnTe alloys using photoluminescence spectroscopy. *Mat. Res. Soc. Symp. Proc.* 1990. **161**. P. 39–44.
6. Johnson S.M., Sen S., Konkel W.H., Kalisher M.H. Optical technique for composition measurement of bulk and thin-film $Cd_{1-x}Zn_xTe$. *J. Vac. Sci. Technol. B*. 1991. **9**, No. 3. P. 1897–1901.
7. Gonzales-Hernandez J., Zylaya O., Mendoza-Alverez J.G. Structural and optical characterization of $Zn_xCd_{1-x}Te$ thin films prepared by the close spaced vapor transport method. *J. Vac. Sci. Technol. A*. 1991. **9**, No. 3. P. 550–553.
8. Oettinger K., Hofmann D.M., Efros Al.L. et al. Excitonic line broadening in bulk grown $Cd_{1-x}Zn_xTe$. *J. Appl. Phys.* 1992. **71**, No. 9. P. 4523–4526.
9. Reno J.L., Jones E.D. Determination of the dependence of the band-gap energy on composition for $Cd_{1-x}Zn_xTe$. *Phys. Rev. B*. 1992. **45**, No. 3. P. 1440–1442.
10. Tobin S.P., Tower J.P., Norton P.W. et al. A comparizon of techniques for nondestructive composition measurements in CdZnTe substrates. *J. Electron. Mater.* 1995. **24**, No. 5. P. 697–705.
11. Poon H.C., Feng Z.C., Feng Y.P., Li M.F. Relativistic band structure of ternary II-VI semiconductor alloys containing Cd, Zn, Se and Te. *J. Phys.: Condens. Matter.* 1995. **7**, No. 14. P. 2783–2799.
12. Toney J.E., Brunett B.A., Schlesinger T.E. et al. Uniformity of $Cd_{1-x}Zn_xTe$ grown by high-pressure Bridgman. *Nucl. Instrum. and Methods in Phys. Res. A*. 1996. **380**, No. 1-2. P. 132–135.
13. Franc J., Hlidek P., Moravec P. et al. Determination of energy gap in $Cd_{1-x}Zn_xTe$ (x = 0–0.06). *Semicond. Sci. Technol.* 2000. **15**, No. 6. P. 561–564.
14. Schlesinger T.E., Toney J.E., Yoon H. et al. Cadmium zinc telluride and its use as a nuclear radiation detector material. *Mater. Sci. Eng. R*. 2001. **32**, No. 4-5. P. 103–189.
15. Glinchuk K.D., Litovchenko N.M., Strilchuk O.N. Analysis of the use of luminescence method for determination of $Cd_{1-x}Zn_xTe$ composition. *Semiconductor Physics, Quantum Electronics and Optoelectronics*. 2003. **6**, No. 2. P. 121–128.
16. Glinchuk K.D., Litovchenko N.M., Prokhorovich A.V., Strilchuk O.N. Analysis of luminescence method for determination of $Cd_{1-x}Zn_xTe$ composition. *Semiconductor Physics, Quantum Electronics and Optoelectronics*. 2005. **8**, No. 3. P. 39–44.
17. Hjelt K., Yuvonen M., Toomi T. et al. Photoluminescence of $Cd_{1-x}Zn_xTe$ crystals grown by high-pressure Bridgeman technique. *phys. status solidi* (*a*). 1997. **162**, No. 2. P. 747–763.
18. Gavrilenko V.I., Grehov A.M., Korbutyak D.V., Litovchenko V.G. *Optical Properties of Semiconductors*. Kyiv: Naukova Dumka, 1987 (in Russian).
19. Korbutyak D.V., Melnichuk S.V., Korbut E.V., Borisyuk M.M. *Cadmium Telluride: Impurity Defect States and Detector Properties*. Kyiv: Publ. House "Ivan Fedorov", 2000 (in Ukrainian).
20. Korbutyak D.V., Krylyuk S.G., Kryuchenko Yu.V., Vakhnyak N.D. Peculiarities of photoluminescence of compensated CdTe:Cl crystals (a review). *Optoelectronics and Semiconductor Technique*. 2002. **37**. P. 23–40 (in Ukrainian).
21. Komar V.V., Nalivaiko D.P., Gerasimenko A.S. *et al.* Growth and characterization of CdZnTe crystals grown by high-pressure Bridgman method in single- and multizone furnaces. *Poverkhnost. Rentgen. synkhrotron. nejtron issledov*. 2002. No. 3. P. 94–99 (in Russian).
22. Tirado-Mejia L., Marin-Hurtado J.I., Ariza-Calderon H. Influence of disorder effects on $Cd_{1-x}Zn_xTe$ optical properties. *phys. status solidi* (*b*). 2000. **220**, No. 1. P. 255–260.
23. Rodriguez M.E., Guttierrez A., Zelaya-Angel O. et al. Influence of crystal quality on the thermal, optical and structural properties of $Cd_{1-x}Zn_xTe$ for low zinc concentration. *J. Cryst. Growth*. 2001. **233**, No. 1-2. P. 275–281.
24. Brunett B.A., Shlesinger T.E., Toney J.E., James R.B. Room-temperature photoluminescence mapping of CdZnTe detectors. *SPIE*. 1999. **3768**. P. 348–358.